Supplementary Information

Preparation of High-Porosity B-TiO_2/C_3N_4 Composite Materials: Adsorption–Degradation Capacity and Photo-Regeneration Properties

Xiang Guo[1], Lei Rao[2,*] and Zhenyu Shi[1]

[1] College of Environment, Hohai University, Nanjing 210098, China; gx2015@hhu.edu.cn

[2] College of Mechanics and Materials, Hohai University, Nanjing 21100, China; raol@hhu.edu.cn

* Correspondence: raol@hhu.edu.cn;

Supplementary Text

The composite B-TiO_2/C_3N_4 of this work was compared previously reported under similar conditions (Table 1). From the above comparison and the performed tests, it can be concluded that the MB adsorption and photocatalytic rate of B-TiO_2/C_3N_4 is enhanced clearly.

Table S1. Comparison of MB removal rate of different materials

Catalysts	Mass of catalyst	Experimental conditions	Removal efficiency	Reference
B-TiO_2/C_3N_4	30 mg	100ml of 20 mg/L MB	73.8%（Dark reaction in 30 min） 97.3%（Light reaction in 2h）	This work
B-C_3N_4	30 mg	100ml of 20 mg/L MB	43.11%（Dark reaction in 30 min）96.8% (Light reaction in 2h)	[1]
H-g-C_3N_4	0.1g	100ml of 1000 mg/L MB	43.23%（Dark reaction in 60 min） 96.61% (Light reaction in 2h)	[2]
Ag-ZnO	0.1%	20ppm	67.3% (Light reaction in 3.5h)	[3]
TiO_2	30mg	100ml of 20 mg/L MB	4.1%（Dark reaction in 30 min） 19.8%（Light reaction in 2h）	This work
g- C_3N_4(650℃)	25mg	50ml of 10 mg/L MB	34.5%（Dark reaction in 60 min） 81.2%（Light reaction in 3h）	[4]

References

1. Guo, X.; Rao, L.; Wang, P.; Zhang, L.; Wang, Y. Synthesis of Porous Boron-Doped Carbon Nitride: Adsorption Capacity and Photo-Regeneration Properties. International Journal of Environmental Research and Public Health 2019, 16, 581, doi:10.3390/ijerph16040581.

2. Feng, J.; Chen, T.; Liu, S.; Zhou, Q.; Ren, Y.; Lv, Y.; Fan, Z. Improvement of g-C_3N_4 Photocatalytic Properties Using the Hummers Method. Journal of Colloid and Interface Science 2016, 479, 1–6, doi:10.1016/j.jcis.2016.06.040.

3. Kwon, D.; Kim, J. Silver-Doped ZnO for Photocatalytic Degradation of Methylene Blue. Korean J. Chem. Eng. 2020, 37, 1226–1232, doi:10.1007/s11814-020-0520-7.

4. Mo, Z.; She, X.; Li, Y.; Liu, L.; Huang, L.; Chen, Z.; Zhang, Q.; Xu, H.; Li, H. Synthesis of g-C_3N_4 at Different Temperatures for Superior Visible/UV Photocatalytic Performance and Photoelectrochemical Sensing of MB Solution. RSC Adv. 2015, 5, 101552–101562, doi:10.1039/C5RA19586A.

Supplementary Figures

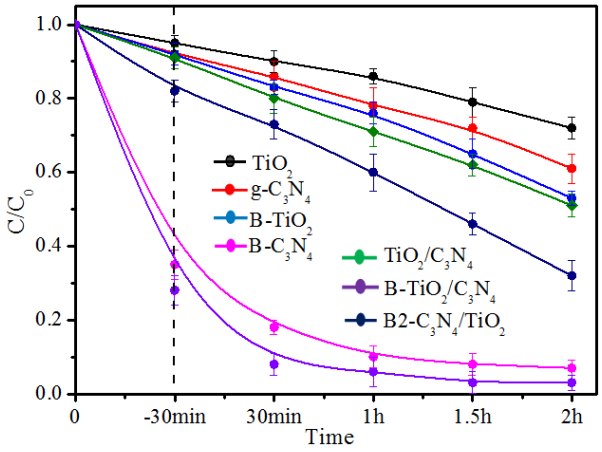

Figure S1. MB removal efficiency of several materials: TiO_2, g-C_3N_4, B-TiO_2, B- C_3N_4, TiO_2/C_3N_4, B2-C_3N_4/TiO_2 and B-TiO_2/C_3N_4.

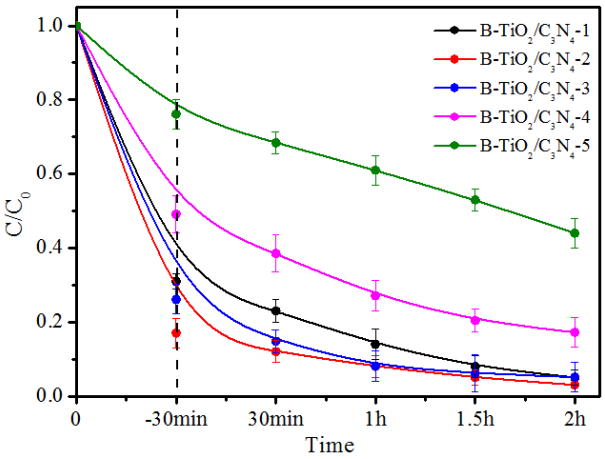

Figure S2. MB removal efficiency of B-TiO_2/C_3N_4 prepared with different doping amount.

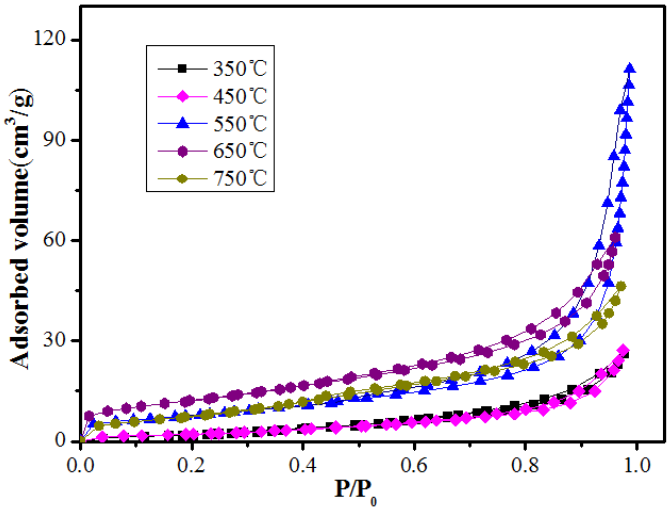

Figure S3. N_2 adsorption-desorption curves of B-TiO_2/C_3N_4 materials at different temperatures.

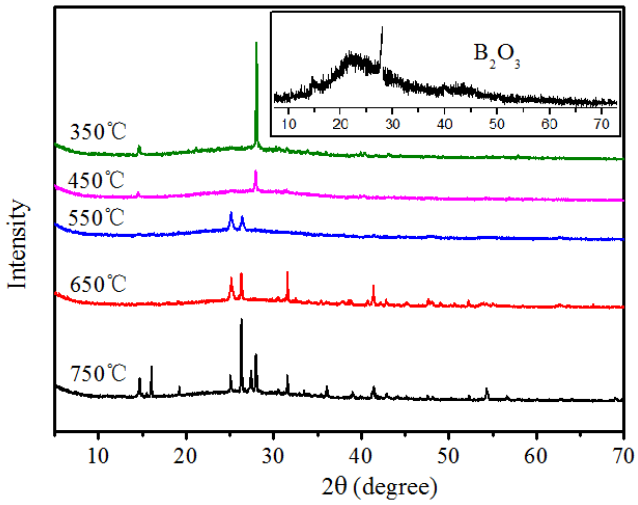

Figure S4. XRD (X-ray diffraction) patterns of B_2O_3 and B-TiO_2/C_3N_4-2 Series materials.

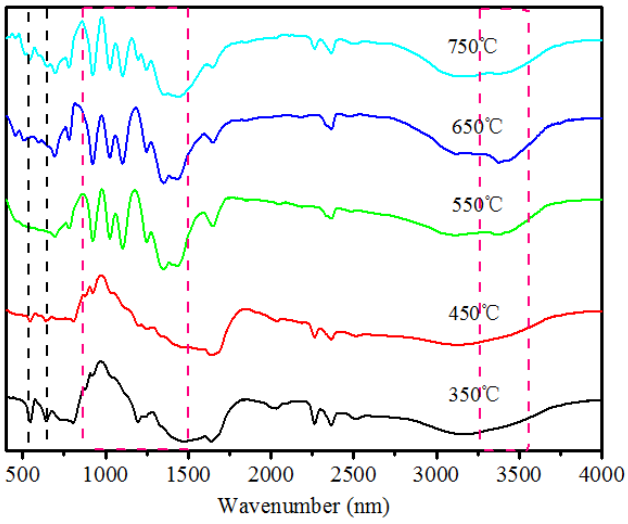

Figure S5. FT-IR spectra for different temperature B-TiO_2/C_3N_4.

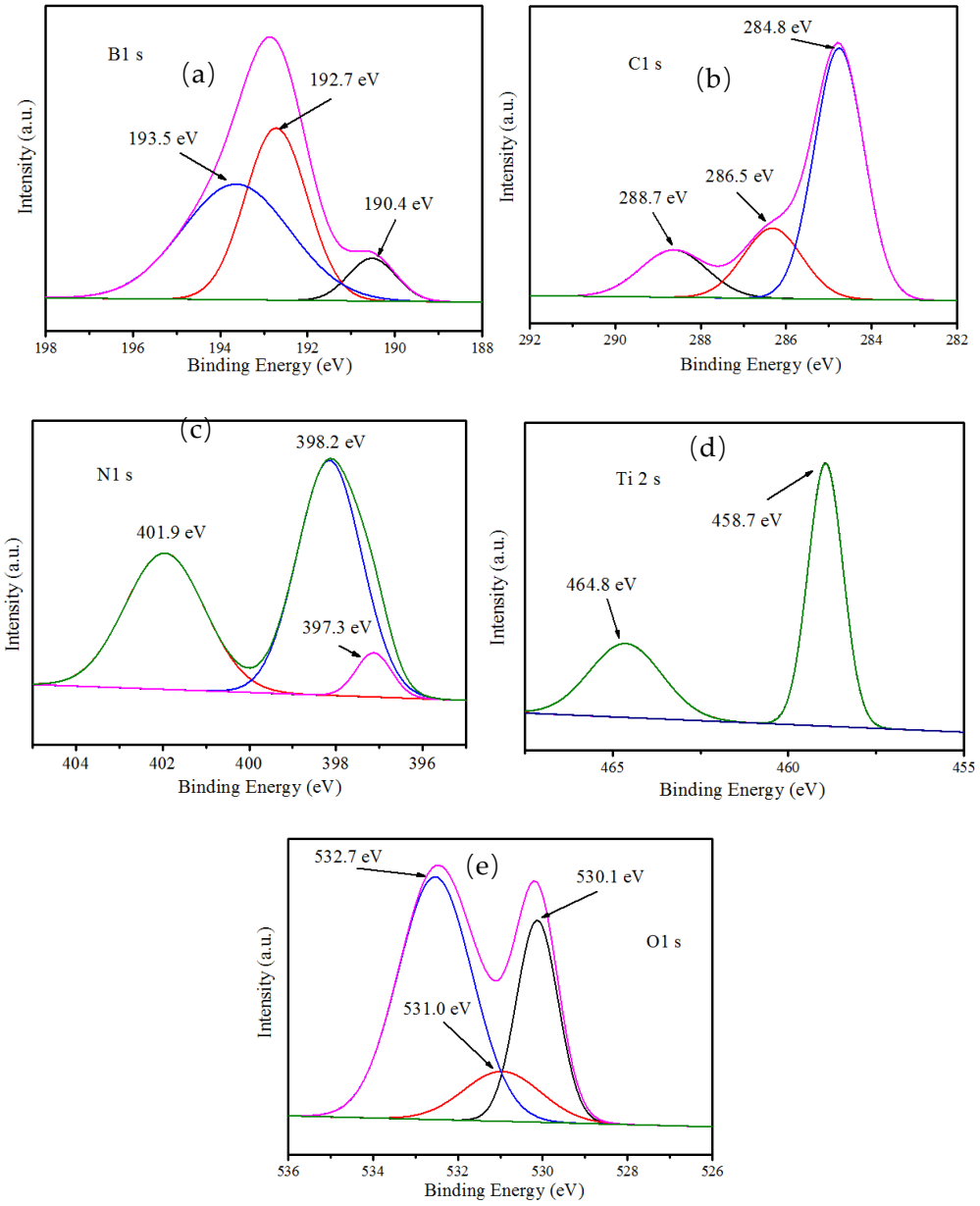

Figure S6. XPS spectra of B-TiO_2/C_3N_4 material (a)B1s, (b)C1s,(c) N1s,(d) Ti2p and (e) O1s.

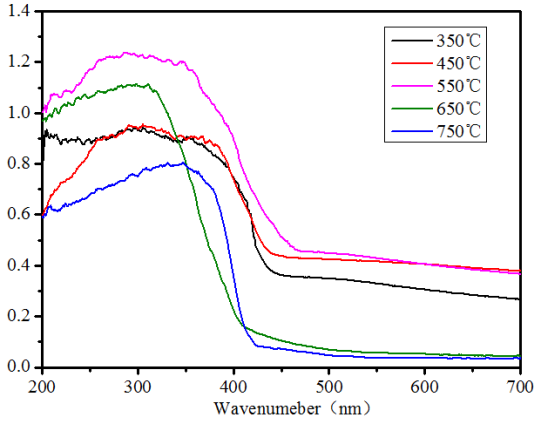

Figure S7. The Diffuse reflectance spectra for different temperature B-TiO_2/C_3N_4

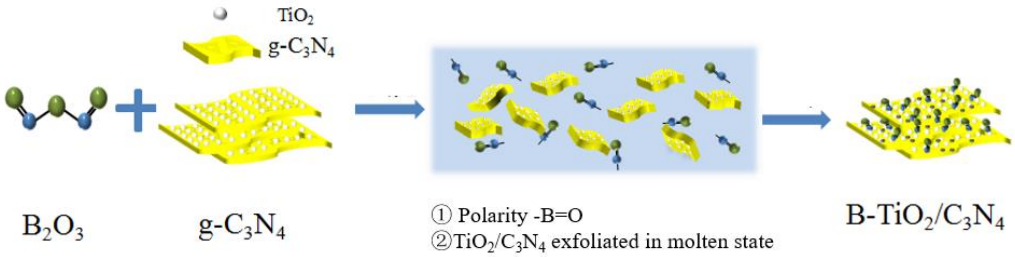

Figure S8. Synthesis path of B-TiO_2/C_3N_4 material

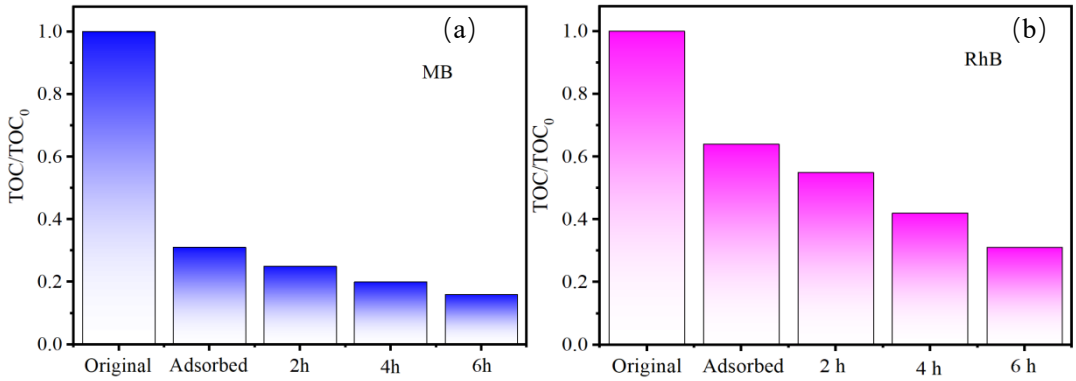

Figure S9. Changes of TOC in the experiment of adsorption-catalytic degradation of pollutants (a) MB (b) RhB